

Experimental Study of Si Monolayers for Future Extremely-Thin SOIs (ETSOIs) : Phonon Confinement Effects and Strain due to Si Bending

T. Mizuno¹, K. Tobe¹, Y. Maruyama¹, and T. Sameshima²

¹Kanagawa University, 2946, Tsuchiya, Hiratsuka 259-1293, Japan (mizuno@info.kanagawa-u.ac.jp)

²Tokyo University of Agriculture and Technology, 2-24-18, Nakamachi, Koganei, Tokyo 184-8588, Japan

I. Introduction

Extremely-thin SOI MOSFETs (ETSOIs) are candidates for future CMOS, because ETSOIs with an intrinsic Si channel can suppress both the short channel effects and the Coulomb scattering of the carriers in the channel [1]. It is also reported that the electron mobility in ETSOIs is affected by the SOI thickness T_{SOI} , because of the quantum-mechanical confinement effects of electrons in ETSOIs [2]. However, the quantum phonon confinement induces the carrier mobility reduction due to the enlarged phonon scattering of carriers [3]. In addition, in low dimensional Si-nanostructures (Si nanowires and nanocrystals) [4], the phonon confinement is enhanced, compared to those of ETSOIs. However, physical limitation of T_{SOI} and a Si monolayer structure have not been studied in detail, yet.

In this work, we have experimentally studied the Si monolayers fabricated by a thermal oxidation technique of the SOI layers. We have successfully formed the Si monolayers with T_{SOI} of about 0.5-nm, evaluated by high-resolution TEM (HRTEM), high-angle annular dark field STEM (HAADF-STEM), and UV/visual reflection spectrum methods. Moreover, we have also discussed the physical limitations of the Si monolayer analyzed by UV-Raman spectroscopy and the HRTEM observations, by showing the experimental data of the strain effects caused by the Si bending and an Raman peak broadening effects due to the phonon confinement in T_{SOI} less than 2.3 nm.

II. Experimental for Si Monolayer

Fig.1 shows the T_{SOI} design as a function of the effective channel length L_{EFF} of ETSOIs to suppress the short channel effects, according to the empirical law of $T_{SOI}=L_{EFF}/3$ [1]. The T_{SOI} should continue to decrease with scaling down of L_{EFF} , and is equal to the lattice constant of Si, a_{Si} (0.54 nm), when $L_{EFF}\approx 1.6$ nm. Therefore, it is necessary to study the Si monolayer with the same T_{SOI} as a_{Si} for future ETSOI-CMOS.

To construct a well-controlled fabrication process for the ETSOIs and the Si monolayers, a (100) SOI substrate is oxidized to be thinned by an internal thermal oxidation technique (ITOX) [5] at 1100 °C for various oxidation time T_O .

The T_{SOI} is mainly evaluated by HRTEM, HAADF-STEM and the UV/visual reflection spectrum. We have analyzed the physical properties of ETSOIs by using a UV-Raman spectroscopy, where the laser beam wavelength is 325 nm, the diameter is about 1 μ m, and the penetration length λ_p in the Si layer is about 5 nm.

III. Si Monolayer Formation

Figs. 2(a) and 2(b) show the TEM and the HRTEM images of the [110] cross section of the Si monolayer, respectively. The T_{SOI} value of 0.56-nm measured by the HRTEM observation is the same as the T_{SOI} of 0.53-nm evaluated by the UV/visual reflection method. Fig. 2(a) shows somewhat T_{SOI} variations in ETSOIs.

The T_{SOI} value is also consistent with the T_{SOI} determined by the HAADF-STEM image, as shown in Fig.3. Fig.3 shows that the experiment dimensions of the Si monolayers (Fig.3(a)) are the same as the simulated image (Fig.3(b)). According to the above T_{SOI} value of about 0.5-nm, it is concluded that we have successfully formed the Si monolayer.

The SBF-STEM image (Fig.4(a)) indicates the clear lattice spots in the whole Si regions, and thus the amorphous Si (*a*-Si) layer was not observed in the Si monolayers. Moreover, the uniform HAADF-STEM image (Fig.4(b)) shows no SiO₂ region formed by oxidizing the whole Si monolayers.

IV. Phonon Confinement

Figs. 5(a)-(c) show the experimental data of UV-Raman spectroscopy in various T_{SOI} conditions. When T_{SOI} is thicker than 5.7 nm at least (Fig. 5(a)), the symmetric Raman peak of

ETSOIs is the same peak as the normal Si (520 cm⁻¹) due to the usual threefold degenerate optical phonon mode. However, when $0.56\text{ nm}\leq T_{SOI}\leq 2.3$ nm, the net Raman peaks (red lines), which subtract the Si intensity I_{Si} of the Si substrates under the BOX from the experimental intensity, show the asymmetric broadening and the downshift. The asymmetric broadening of the Raman peak is enhanced with decreasing T_{SOI} . As discussed in Figs.4, it is clear that the Raman intensity below 500 cm⁻¹ does not originate from the *a*-Si layer. Therefore, the asymmetric broadening of the net Raman peaks is attributable to the quantum phonon confinement [4] in two-dimensional ETSOIs. In addition, some part of the downshift is also due to the phonon confinement, but the main mechanism is caused by the strain effects of the ETSOI layers, as discussed in the next section.

The Raman spectrum of the Si nanowires and nanocrystals with a high heat resistance strongly depends on the laser power [6]. However, Fig.6 shows that the net Raman spectrum of the Si monolayers is independent on the laser power P_L , when $P_L\leq 1\text{ mW}$.

Moreover, Fig. 7 shows the 2D mapping data for the Raman downshift $\Delta\omega$ of the Si monolayers below the 520cm⁻¹ Si peak in 150- μ m squares area. The $\Delta\omega$ varies widely, and the average and the standard deviation are 7.8 cm⁻¹ and 1.7 cm⁻¹, respectively. The $\Delta\omega$ variation is mainly caused by the variations of the T_{SOI} and the Si monolayer bending, as discussed in the next section.

V. Strain due to Si Bending

Figs. 8(a) and 8(b) show the $\Delta\omega$ and the FWHM values of the net Raman peaks of ETSOIs as a function of T_{SOI} . Both the $\Delta\omega$ and the FWHM suddenly increases at the critical T_{SOI} value of 2.3 nm and continues increasing with decreasing T_{SOI} . Therefore, the phonon confinement effects and the tensile strain value into the ETSOIs increase with decreasing T_{SOI} . In addition, Fig. 8(a) indicates that $\Delta\omega\propto -3.8\ln(T_{SOI})$. Thus, the standard deviation of T_{SOI} , ΔT_{SOI} of the Si monolayer in the 150- μ m square area is about 0.25-nm, according to the $\Delta\omega$ variation in Fig. 7. The relative large ΔT_{SOI} is the first physical limitation of the Si monolayer in this study.

Here, we discuss the physical model for introducing the tensile strain into the ETSOIs. We have observed the Si monolayer bending, as shown as the HRTEM image in Fig.9. The maximum Si bending is 0.44nm in this area. In addition, the horizontal length a of the lateral 15 Si atoms is 5.70 nm. On the other hand, the slope length b of the lateral 15 Si atoms is 5.74 nm. As a result, the Si monolayers in the bending region are tensile strained and the maximum strain value ($b-a/a$) is about 0.7%. Therefore, the $\Delta\omega$ due to the maximum strain in this area corresponds to 6cm⁻¹, and so can explain about 77% of the experimental $\Delta\omega$ value (7.8cm⁻¹) shown in Fig.7(a). Thus, some part of the $\Delta\omega$ value is attributable to the downshift due to the phonon confinement. Moreover, Fig.8(a) indicates that the Si bending increases with decreasing T_{SOI} , which is considered to be due to the oxide layer stress into the ETSOIs. The Si bending is the second physical limitation of the Si monolayer in this study.

VI. Conclusion

We have experimentally studied Si monolayers for future ETOI CMOS which was fabricated by the ITOX process. We have successfully formed the 0.56-nm Si monolayers confirmed by HRTEM, HAADF-STEM, and a UV/visual reflection method. We have demonstrated the quantum phonon confinement and the Si bending of the Si monolayers evaluated by the UV-Raman spectroscopy. Therefore, it is necessary to consider the carrier mobility reduction due to the quantum phonon dispersion effects in two dimensional ETSOIs, to design the future ETSOI-CMOS.

References: [1] M.Yoshimi, IEICE Trans., E74, 337, 1991. [2] K.Uchida, IEDM, p.47, 2002. [3] L.Donetti, J.Appl.Phys., 100, 013701, 2006. [4] K.W.Adu, in *Nanosilicon*, ed. V.Kumar, (Elsevier, 2008), Chap.7. [5] S. Nakashima, J. Electrochem. Soc. **143**, 244, 1996. [6] S. Piscanec, Phys.Rev.B, 68, 241312(R), 2003.

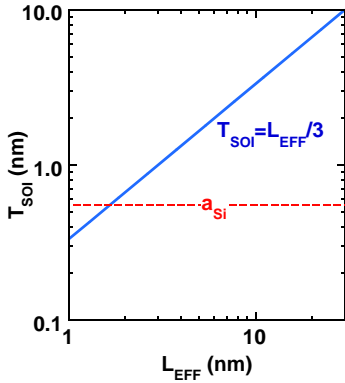


Fig.1 Scaling for T_{SOI} in ETSOIs, using $T_{SOI} = L_{EFF}/3$ [1]. a_{Si} is the lattice constant of Si.

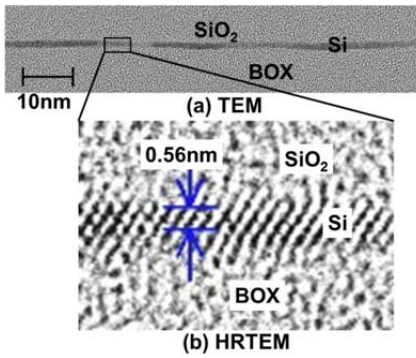


Fig.2 0.56-nm Si monolayers evaluated by (a) TEM (Transmission Electron Microscopy) observations and (b) HRTEM images of the [110] cross section of the Si monolayers, respectively. Fig.(a) shows T_{SOI} variations and small Si bending.

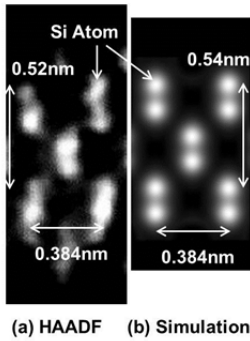


Fig.3 (a) HAADF image of STEM (Scanning TEM) observation and (b) the simulated Si atom image of the [110] cross section of the Si monolayers. The white spots show the Si atoms, and the experimental a_{Si} (0.52-nm) in Fig.(a) is almost the same as the simulated result (0.54-nm) in Fig.(b).

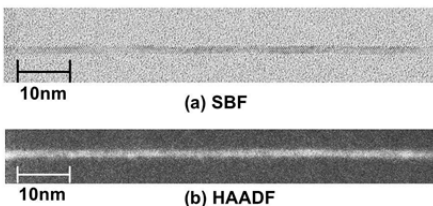


Fig.4 (a) SBF (Scanning Bright Field) image and (b) HAADF image of STEM observation of the [110] cross section of the Si monolayers at the same area.

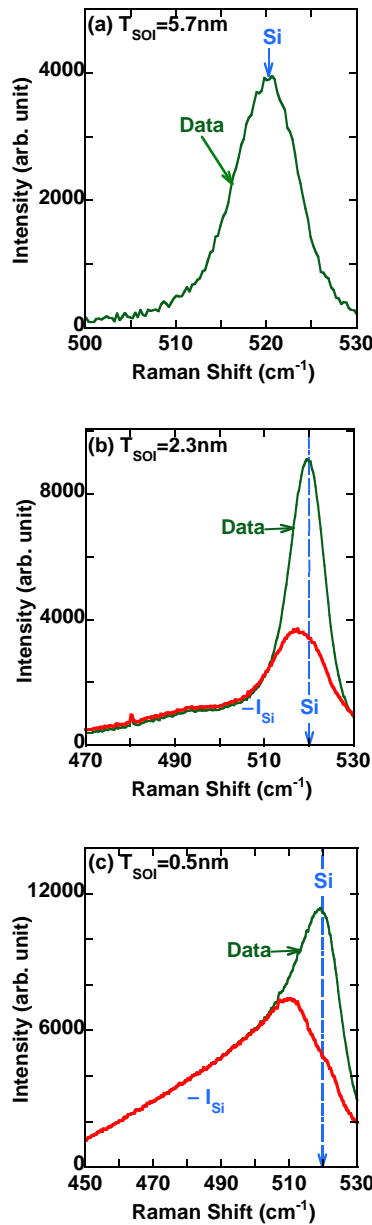


Fig.5 UV Raman spectra of Si layers with (a) $T_{SOI}=5.7\text{nm}$, (b) $T_{SOI}=2.3\text{nm}$, and (c) $T_{SOI}=0.5\text{nm}$, where the laser power P_L is 1mW. The Si peaks in Figs. (b) and (c) originate from the Si substrate intensity I_{Si} under the BOX, because $\lambda_p > T_{SOI}$. The green and the red lines show the experimental data and the net intensity of the Si layers on the BOX which subtract I_{Si} from the data, respectively.

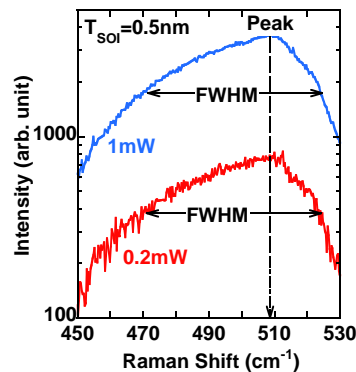


Fig.6 Laser power dependence of the net Raman spectra of Si monolayers. The blue and the red lines show the data of P_L of 1 mW and 0.2 mW, respectively.

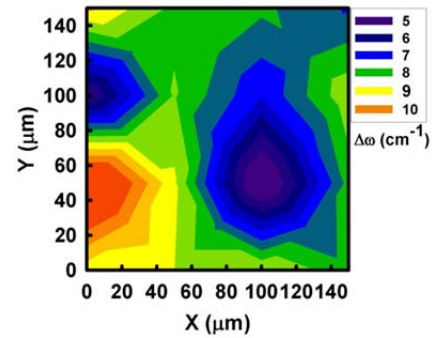


Fig.7 2D mapping (150μm squares) of Raman shift data $\Delta\omega$ of Si monolayers from the Si peak of 520cm^{-1} , where P_L is 1mW. The average $\Delta\omega$ and the standard deviation of the $\Delta\omega$ are 7.8cm^{-1} and 1.7cm^{-1} , respectively.

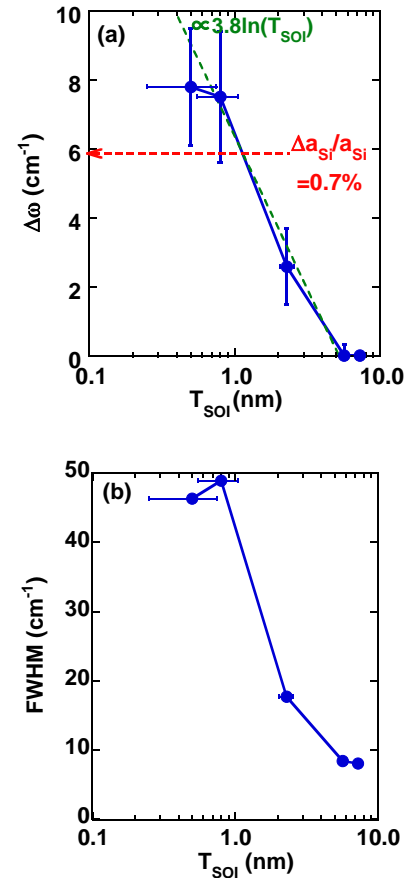


Fig.8 T_{SOI} dependence of (a) $\Delta\omega$ and (b) FWHM (Full Width Half Maximum) value of the Raman peak broadening, where P_L is 1mW. The dashed arrow in Fig.(a) shows the calculated $\Delta\omega$ due to the tensile strain value caused by the maximum Si monolayer bending shown in Fig.9. The dashed line of $\Delta\omega \propto \ln(T_{SOI})$ shows fitting curve of the data in $1.4\text{-nm} \leq T_{SOI} \leq 5.7\text{-nm}$.

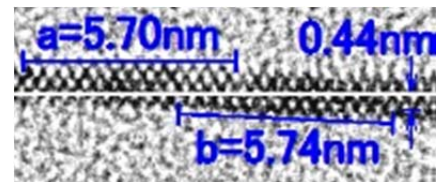


Fig.9 HRTEM image of the [110] cross section of the Si monolayer bending. The solid white line shows the horizontal Si/BOX interface. The Si bending (arrows) was 0.44nm . As a result, the horizontal length a of the lateral 15 Si atoms is 5.70nm , resulting in the 0.38nm space between lateral two Si atoms. However, the slope length b of the lateral 15 Si atoms is 5.74nm . As a result, the Si monolayers are tensilely strained and the strain value is about 0.7%.